Mathematisch-Naturwissenschaftliche Fakultät
Ernst Moritz Arndt Universität Greifswald

Bachelor Thesis

Theory and Modeling of Gyroscopes

Karl Felix Lüskow
Greifswald, July 10, 2011

Gutachter:
Prof. Dr. Ralf Schneider
PD Dr. Berndt Bruhn

Contents

1 Motivation

As a child nearly everybody has played with a spinning top and was fascinated to see how it spins. Imagine now this spinning top would start to float due to some force. This is exactly what a levitron is doing, using a magnetic force counteracting gravity to allow for levitation. It is rather tricky to operate it successfully and can take hours or days of frustrating trials. After several attempts, it really is a magic moment, when the spinning top is levitating for some seconds. Several physicists studied this system in detail and tried to analyze its operational principle. The physics of levitrons is

Figure 1.1: A photo of a levitron [1]

similar to magnetostatic traps of neutral atoms [2] or ion traps. There it is important to analyze the trajectories of charged particles trapped in force fields.
The intention of this work is to find solutions for the movement of a levitron. After a short summary of the fundamental principles for the movement of rigid bodies, the Hamiltonian will be calculated after formulating the kinetic and the potential energy. To solve the equations of motions two different numerical methods will be discussed. Identifying an invariant set of the equations of motion allows a considerable reduction of the dimension of the problem. This reduced set of equations is then used to analyse the operational space numerically and to find analytical solutions with a linearization approach. This allows to quantify conditions under which a stable levitation of the top is possible. Finally, the work is summarised.

2 Theoretical background

M.V. Berry [3] showed, that there is a rather limited operational space to get a levitating top with a minimum frequency to allow for a stable levitation. T.B. Jones, M. Washizu and R. Gans [4] made experiments and compared them with their theoretical calculations. They proved that there cannot be any stable solution for a top, when it is "rigidly aligned with the vertical axis". A small tilt of the rotation axis is needed. They claimed that the locus is only 4mm in length and that the mass of the top must be within a 1% margin. They also found an upper and a lower limit for the rotation frequency of the top. Numerical solutions [5] were presented for the full equations of motions and some solutions for stable and instable trajectories were shown. H.R. Dullin [6] developed an improved model of a levitron. He found an invariant set of equations which reduce the system to a four dimensional problem. He also determined the critical spin rates using a linearization approach. The work presented in this thesis follows mostly these publications trying to combine analytical and numerical results for a better understanding of the system.

2.1 Kinematics

The dynamics of a levitron is determined by the theory of kinetics of spinning tops. The top is described as a rigid body. In the following the different elements needed for the theoretical description are introduced and discussed. The kinetic energy is independent of the magnetic field. It can be split into two contributions: a translation of the center of mass (cm) and a rotation about an axis.
The translational energy of the center of mass is

$$T_{trans} = \frac{1}{2} m v_{cm}^2 = \frac{1}{2} m \left(\dot{x}_{cm}^2 + \dot{y}_{cm}^2 + \dot{z}_{cm}^2 \right) , \tag{2.1.1}$$

where $\dot{x}$, $\dot{y}$ and $\dot{z}$ are the velocities in the x-,y- and z-direction of the space, respectively. For the calculation of the rotation, the first step is to analyze a simple rotation

of a vector $\vec{G}(t)$.

$$(d\vec{G})_{space} = (d\vec{G})_{body} + (d\vec{G})_{rot} \tag{2.1.2}$$

In the case of a rigid body, $\vec{G}$ is constant in body coordinates, therefore

$$(d\vec{G})_{space} = (d\vec{G})_{rot} = d\vec{\Omega} \times \vec{G}\,, \tag{2.1.3}$$

where $d\vec{\Omega}$ describes the differential vector angle belonging to the rotation. Defining $\vec{\omega}$ as the angular velocity $\frac{d\vec{\Omega}}{dt}$ it follows

$$\frac{d\vec{G}_{rot}}{dt} = \vec{\omega} \times \vec{G}\,. \tag{2.1.4}$$

The angular velocity $\vec{\omega}$ can be expressed by Euler angles (see Goldstein for defintion of the angles [7]).

$$\vec{\omega}_\phi = \begin{pmatrix} 0 \\ 0 \\ \dot{\phi} \end{pmatrix} \qquad \vec{\omega}_\theta = \begin{pmatrix} \dot{\theta}\cos\phi \\ \dot{\theta}\sin\phi \\ 0 \end{pmatrix} \qquad \vec{\omega}_\psi = \begin{pmatrix} 0 \\ 0 \\ \dot{\psi} \end{pmatrix} \tag{2.1.5}$$

The angular velocity along the z-axis of the system is denoted by ω_ϕ, ω_θ along the line of nodes and ω_ψ is along the z'-axis. These three components of the angular velocity need to be transformed into body coordinates. For this, the vectors are multiplied with a rotation matrix, which can transform any vector in body coordinates.

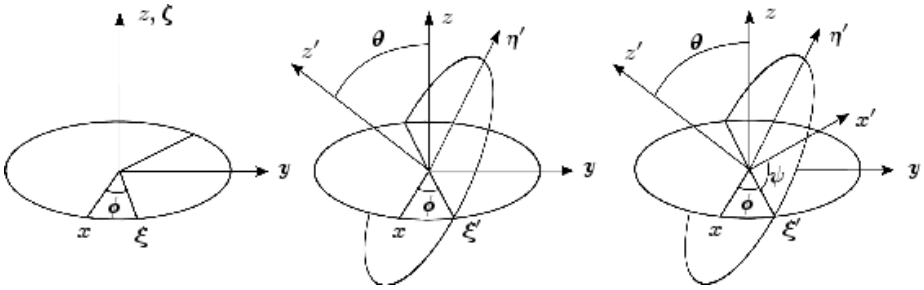

Figure 2.1: definition of Euler angles [8]

Following Goldstein, this transformation matrix is the product of three rotations. At first the coordinate system is turned anti-clockwise through the angle ϕ around the z-axis (matrix $\mathbf{R}_1$). The new system is turned clockwise through an angle θ around the ξ'-axis (matrix $\mathbf{R}_2$). In the last step the system is rotated anti-clockwise through an angle of ψ around the resulting z'-axis (matrix $\mathbf{R}_3$). The complete transformation

matrix is given by multiplication of these three matrices:

$$\mathbf{R}_1 = \begin{pmatrix} \cos\phi & \sin\phi & 0 \\ -\sin\phi & \cos\phi & 0 \\ 0 & 0 & 1 \end{pmatrix} \tag{2.1.6}$$

$$\mathbf{R}_2 = \begin{pmatrix} 1 & 0 & 0 \\ 0 & \cos\theta & \sin\theta \\ 0 & -\sin\theta & \cos\theta \end{pmatrix} \tag{2.1.7}$$

$$\mathbf{R}_3 = \begin{pmatrix} \cos\psi & \sin\psi & 0 \\ -\sin\psi & \cos\psi & 0 \\ 0 & 0 & 1 \end{pmatrix} \tag{2.1.8}$$

resulting in

$$\mathbf{R} = \mathbf{R}_3\mathbf{R}_2\mathbf{R}_1 = \begin{pmatrix} \cos\psi\cos\phi - \cos\theta\sin\phi\sin\psi & \cos\psi\sin\phi + \cos\theta\cos\phi\sin\psi & \sin\psi\sin\theta \\ -\sin\psi\cos\phi - \cos\theta\sin\phi\cos\psi & -\sin\psi\sin\phi + \cos\theta\cos\phi\cos\psi & \cos\psi\sin\theta \\ \sin\theta\sin\phi & -\sin\theta\cos\phi & \cos\theta\,. \end{pmatrix}. \tag{2.1.9}$$

This gives the angular velocity in body coordinates:

$$\vec{\omega}' = \mathbf{R}\vec{\omega}_\phi + \mathbf{R}\vec{\omega}_\theta + \mathbf{R}\vec{\omega}_\psi = \begin{pmatrix} \dot{\phi}\sin\theta\sin\psi + \dot{\theta}\cos\psi \\ \dot{\phi}\cos\psi\sin\theta - \dot{\theta}\sin\psi \\ \dot{\phi}\cos\theta + \dot{\psi} \end{pmatrix}. \tag{2.1.10}$$

Using this, one obtains the kinetic energy as the sum of translation and rotation. In the following a superscript T means the transpose of the vector.

$$T = \frac{1}{2}mv_{cm}^2 + \frac{1}{2}\vec{\omega}'^T\ \mathbf{I}\ \vec{\omega}' \tag{2.1.11}$$

with the inertial tensor $\mathbf{I}$ given by

$$\mathbf{I} = \int_V \rho(\vec{r})(r^2\delta_{a,b} - x_a x_b)\ dV\,. \tag{2.1.12}$$

Due to the x-y-symmetry of the levitron, the inertial tensor is constant in body

coordinates and can be written as

$$\mathbf{I} = \begin{pmatrix} A & 0 & 0 \\ 0 & A & 0 \\ 0 & 0 & C \end{pmatrix} . \tag{2.1.13}$$

$A = 2,2\ 10^{-6}\text{kgm}^2$ and $C = 1,32\ 10^{-6}\text{kgm}^2$ are the principal moments of inertia [9]. Finally the kinetic energy is calculated as

$$T = \frac{1}{2}\left[m(\dot{x}^2 + \dot{y}^2 + \dot{z}^2) + A(\dot{\theta}^2 + \dot{\phi}^2 \sin^2\theta) + C(\dot{\psi} + \dot{\phi}\cos\theta)^2\right] . \tag{2.1.14}$$

2.2 Magnetostatic Potential

The potential energy U of the levitron is given by the sum of the gravitational energy and the interaction potential of the magnetic levitron in the magnetic field of the base plate

$$U = mgz - \langle \vec{B}(r), \mu\mathbf{R}\vec{e}_z \rangle , \tag{2.2.1}$$

where μ is the magnetic moment of the levitron.
For a magnetostatic problem the magnetic field $\vec{B}(\vec{r})$ can be calculated from a scalar potential φ with $\vec{B}(\vec{r}) = -\nabla\varphi(\vec{r})$. Using the nabla operator on both sides of the equation and with the Maxwell's equation $\nabla B = 0$ one gets Laplace's equation $\Delta\varphi = 0$, which has to be fulfilled by the scalar potential.
Due to the cylindric symmetry of the levitron, one can expand the potential $\varphi(\vec{r})$ [6] using a Taylor expansion in r:

$$\varphi(r, z) = \varphi_0(z) + r\varphi_1(z) + r^2\varphi_2(z) + \dots \tag{2.2.2}$$

with $r^2 = x^2 + y^2$. Using Laplace's equation, one gets:

$$\Delta\varphi(r) = \varphi_0''(z) + r\varphi_1''(z) + \varphi_1(z)\Delta r + r^2\varphi_2''(z) + \varphi_2(z)\Delta r^2 + \dots = 0 . \tag{2.2.3}$$

The relation $\Delta r^n = n^2 r^{n-2}$ will be used in the following, which can be proven easily:

$$\begin{aligned}\Delta r^n &= \left(\frac{\partial^2}{\partial x^2} + \frac{\partial^2}{\partial y^2} + \frac{\partial^2}{\partial z^2}\right)\left(x^2+y^2\right)^{n/2} \\ &= 2n\left(x^2+y^2\right)^{n/2-1} + 2n\left(\frac{n}{2}-1\right)\left(x^2+y^2\right)^{\frac{n-4}{2}}\left(x^2+y^2\right) \\ &= 2nr^{n-2} + 2n\left(\frac{n}{2}-1\right)r^{n-2} = n^2 r^{n-2}\end{aligned}$$

Arranging equation (2.2.3) to same orders of r and setting them separately to zero results in:

$$\varphi_1 = 0 \qquad \varphi_3 = -\frac{1}{9}\varphi_1'' \qquad \varphi_5 = -\frac{1}{25}\varphi_3'' \tag{2.2.4}$$

$$\varphi_2 = -\frac{1}{4}\varphi_0'' \qquad \varphi_4 = -\frac{1}{16}\varphi_2'' \qquad \varphi_6 = -\frac{1}{36}\varphi_4''\,. \tag{2.2.5}$$

As a consequence of the first equation, all φ_i with odd i are equal zero. For even i it holds that $\varphi_{2i+2} = -(1/(2i+2)^2)\varphi_{2i}''$. Substituting $\Phi_k(z) = \frac{d^k}{dz^k}\varphi_0(z)$ one gets

$$\varphi(r,z) = \Phi_0(z) - \frac{r^2}{4}\Phi_2(z) \pm \dots\,. \tag{2.2.6}$$

$B(r)$ can be expressed up to second order in terms of $\Phi_k(z)$:

$$B(r) = -\nabla\varphi(r) = \begin{pmatrix} \frac{x}{2}\Phi_2(z) \\ \frac{y}{2}\Phi_2(z) \\ -\Phi_1(z) + \frac{r^2}{4}\Phi_3(z) \end{pmatrix}. \tag{2.2.7}$$

Following Jackson [10] the general expression for the scalar magnetic potential is

$$\varphi(r) = -\nabla\int_V \frac{M(r')}{|r-r'|}d^3r' \tag{2.2.8}$$

with M as the magnetization of the base plate and volume V. With regards to the geometry of the levitron (with a planar base plate), there is only a magnetic charge density in one z-plane, so that $M(r) = \rho(r)\delta(z)$, where δ denotes the delta distribution. This gives:

$$\varphi = -\nabla\int_V \frac{\rho(r)\delta(z)}{(r^2+z^2)^{1/2}}dz\,d^2r\,. \tag{2.2.9}$$

Integration over z results in

$$\varphi = z \iint_{Base} \frac{\rho(r)}{(r^2+z^2)^{3/2}} d^2r \,. \tag{2.2.10}$$

In this work, a disk of radius a with a hole of radius w is used to calculate the form of the scalar potential. Therefore the integral is solved in polar coordinates:

$$\varphi = 2\pi z \int_{r=w}^{a} \frac{r\rho(r)}{(r^2+z^2)^{3/2}} dr = 2\pi z\rho \left(\frac{1}{\sqrt{z^2+w^2}} - \frac{1}{\sqrt{z^2+a^2}} \right) . \tag{2.2.11}$$

ρ can be taken out of the integration, because it is constant for $w < z < a$.
Of course there are other possibilities to describe the magnetic base plate, depending on its exact geometry. But according to the work of Berry [3] the resulting differences in the magnetic fields are small for such different geometries of levitrons like a disc, a square plate or a disc with a central hole.
In order to compute the potential energy given by equation (2.2.1) the magnetic field is needed and it depends on the first three spatial derivatives of the scalar potential (2.2.7). These derivatives are given by:

$$\Phi_1 = 2\pi\rho \left(\frac{1}{\sqrt{z^2+w^2}} - \frac{1}{\sqrt{z^2+a^2}} \right) + 2\pi\rho z \left(\frac{z}{(z^2+a^2)^{\frac{3}{2}}} - \frac{z}{(z^2+w^2)^{\frac{3}{2}}} \right) \tag{2.2.12}$$

$$\begin{aligned} \Phi_2 = {} & 4\,\pi\,\rho \left(\frac{z}{(z^2+d^2)^{\frac{3}{2}}} - \frac{z}{(z^2+w^2)^{\frac{3}{2}}} \right) \\ & + 2\,\pi\,\rho\,z \left(-\frac{1}{(z^2+w^2)^{\frac{3}{2}}} + \frac{3\,z^2}{(z^2+w^2)^{\frac{5}{2}}} + \frac{1}{(z^2+d^2)^{\frac{3}{2}}} - \frac{3\,z^2}{(z^2+d^2)^{\frac{5}{2}}} \right) \end{aligned} \tag{2.2.13}$$

$$\begin{aligned} \Phi_3 = {} & 6\,\pi\,\rho \left(-\frac{1}{(z^2+w^2)^{\frac{3}{2}}} + \frac{3\,z^2}{(z^2+w^2)^{\frac{5}{2}}} + \frac{1}{(z^2+d^2)^{\frac{3}{2}}} - \frac{3\,z^2}{(z^2+d^2)^{\frac{5}{2}}} \right) \\ & + 2\,\pi\,\rho\,z \left(\frac{9\,z}{(z^2+w^2)^{\frac{5}{2}}} - \frac{15\,z^3}{(z^2+w^2)^{\frac{7}{2}}} - \frac{9\,z}{(z^2+d^2)^{\frac{5}{2}}} + \frac{15\,z^3}{(z^2+d^2)^{\frac{7}{2}}} \right) \end{aligned} \tag{2.2.14}$$

With this scalar potential one is able to find the B-field and the expression for the potential energy

$$U = mgz - \mu(\sin\psi\sin\theta B_x + \cos\psi\sin\theta B_y + \cos\theta B_z) \,. \tag{2.2.15}$$

2.3 Hamiltonian

Knowing the kinetic and the potential energy one is able to formulate the Lagrangian:

$$\begin{aligned}\mathcal{L} =& T(\dot{x}^2, \dot{y}^2, \dot{z}^2) - U(x, y, z) \\ =& \frac{1}{2}\left[m(\dot{x}^2 + \dot{y}^2 + \dot{z}^2) + A(\dot{\theta}^2 + \dot{\phi}^2 \sin^2\theta) + C(\dot{\psi} + \dot{\phi}\cos\theta)^2\right] \\ &+ \mu\left[\sin\theta\sin\psi B_x + \sin\theta\cos\psi B_y + \cos\theta B_z\right] - mgz \end{aligned} \tag{2.3.1}$$

The Lagrangian equations of motion define the generalized coordinates:

$$p_x = \frac{\partial \mathcal{L}}{\partial \dot{x}} = m\dot{x} \tag{2.3.2}$$

$$p_y = \frac{\partial \mathcal{L}}{\partial \dot{y}} = m\dot{y} \tag{2.3.3}$$

$$p_z = \frac{\partial \mathcal{L}}{\partial \dot{z}} = m\dot{z} \tag{2.3.4}$$

$$p_\theta = \frac{\partial \mathcal{L}}{\partial \dot{\theta}} = A\dot{\theta} \tag{2.3.5}$$

$$p_\psi = \frac{\partial \mathcal{L}}{\partial \dot{\psi}} = C(\dot{\psi} + \dot{\phi}\cos\theta) \tag{2.3.6}$$

$$p_\phi = \frac{\partial \mathcal{L}}{\partial \dot{\phi}} = A\dot{\phi}\sin^2\theta + C(\dot{\psi} + \dot{\phi}\cos\theta)\cos\theta \tag{2.3.7}$$

The time derivatives $\dot{q}_i$ can be written in a 6-dimensional vector form:

$$\begin{aligned}\vec{\dot{q}} =& (\dot{x}; \dot{y}; \dot{z}; \dot{\theta}; \dot{\psi}; \dot{\phi}) \\ =& \left(\frac{p_x}{m}; \frac{p_y}{m}, \frac{p_z}{m}; \frac{p_\theta}{A}; \frac{p_\psi}{C} - \frac{p_\phi\cos\theta - p_\psi\cos^2\theta}{A\sin^2\theta}; \frac{p_\phi - p_\psi\cos\theta}{A\sin^2\theta}\right) \end{aligned} \tag{2.3.8}$$

The Hamiltonian $\mathcal{H}$ is calculated as

$$\begin{aligned}\mathcal{H} =& \vec{\dot{q}}^T\vec{p} - \mathcal{L} \\ =& \frac{1}{2m}\left(p_x^2 + p_y^2 + p_z^2\right) + \frac{p_\theta^2}{2A} + \frac{p_\psi^2}{2C} + \frac{\left(p_\phi - p_\psi\cos\theta\right)^2}{2A\sin^2\theta} \\ &+ \mu\left[\sin\theta\sin\psi\frac{\partial\varphi}{\partial x} + \sin\theta\cos\psi\frac{\partial\varphi}{\partial y} + \cos\theta\frac{\partial\varphi}{\partial z}\right] + mgz\,. \end{aligned} \tag{2.3.9}$$

Then the derivatives of the generalized momenta follow from

$$\dot{p}_q = -\frac{\partial \mathcal{H}}{\partial q}\,. \tag{2.3.10}$$

The calculation of the derivatives of the generalized coordinates results in the same expressions like with the Lagrangian. For the momenta one gets:

$$\dot{p}_x = -\partial_x U \tag{2.3.11}$$

$$\dot{p}_y = -\partial_y U \tag{2.3.12}$$

$$\dot{p}_z = -\partial_z U \tag{2.3.13}$$

$$\dot{p}_\theta = -\frac{p_\psi \left(p_\phi - p_\psi \cos\theta\right)}{A \sin\theta} + \frac{\cos\theta (p_\phi - p_\psi \cos\theta)^2}{A \sin^3\theta} - \partial_\theta U \tag{2.3.14}$$

$$\dot{p}_\psi = -\partial_\psi U \tag{2.3.15}$$

$$\dot{p}_\phi = 0\,. \tag{2.3.16}$$

The full set of equations of motion are calculated with the computer algebra system wxMaxima.

3 Solving the equations of motion

3.1 ODE Solvers

Due to the complex expressions of the magneto static potential describing the magnetic field, it is impossible to solve the equations of motion without approximations in an analytic form. However, one can use computational methods to solve this system of ordinary differential equations (ODEs). In this work two different solvers were tested and used. The first is the Euler method, which is the simplest one. The other method is named after the two German mathematicians Carl Runge and Martin Wilhelm Kutta. Actually Runge-Kutta describes a whole family of ODE solvers, but in this work the common fourth-order Runge-Kutta algorithm is applied. In the next section these two algorithms will be described in detail.

3.1.1 Euler-Method

The Euler-method [11] is an explicit first order numerical method to find a solution for an ordinary differential equation (ODE) with initial values. For each time step the slope of the function determining the time-derivative is calculated by two points. If the first point is known from the initial condition, one will be able to calculate the slope of the first step. With this value one can find the point at the time $t+h$. With h as a defined time step.
To formulate this in a mathematical way, one tries to find a solution for an ODE:

$$y'(t) = f\left(t, y(t)\right) \tag{3.1.1}$$

with the initial value $f(t_0) = y_0$. The next point for every time step will be calculated by its successor using a linear approximation

$$y_{n+1} = y_n + hf(t_n, y_n)\,, \tag{3.1.2}$$

while the new time is $t_{n+1} = t_n + h$. This method is represented in the picture 3.1.

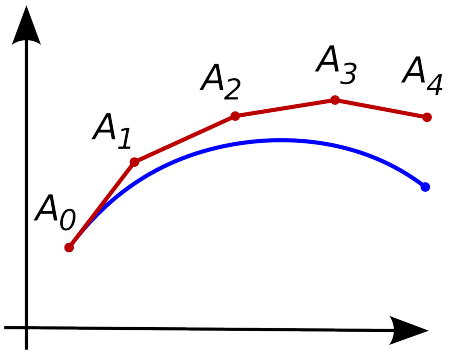

Figure 3.1: scheme of the Euler algorithm [12].

The quality of this algorithm depends strongly on the chosen time step and the particular system. To allow for larger time steps other methods are needed.

3.1.2 Runge-Kutta method

Runge-Kutta-methods are a whole family of ODE solvers. In this work, the common fourth-order Runge-Kutta method [11] is used. Similar to the Euler method every solution for a new time step is calculated by its successor. The difference between the Euler and the Runge-Kutta method is only the way of finding the slope for the next step. In contrast to the Euler method, that uses only one point, the Runge-Kutta method uses 4 different points for the time advance improving the accuracy considerably. Algorithmically, this is expressed in the following way. Here, the same naming conventions are used as for the description of the Euler method:

$$y_{n+1} = y_n + \frac{h}{6}\left(a + 2b + 2c + d\right) \tag{3.1.3}$$

with the coefficients defined as follows

$$\begin{aligned} a &= hf(t_n, y_n) \\ b &= hf\left(t_n + \frac{1}{2}h, y_n + \frac{1}{2}a\right) \\ c &= hf\left(t_n + \frac{1}{2}h, y_n + \frac{1}{2}b\right) \\ d &= hf(t_n + h, y_n + c)\,. \end{aligned} \tag{3.1.4}$$

A comparison between Euler and Runge-Kutta method will be shown in the following section.

3.1.3 Comparison of Euler method and Runge-Kutta method

In this section the accuracy of the Runge-Kutta and Euler method will be analyzed. One compares the Taylor expansion of y in h at t_0

$$y(t_0 + h) = y_0 + hy'(t_0) + \frac{1}{2}h^2 y''(t_0) + O(h^3) \tag{3.1.5}$$

with the equation of the Euler method. Inserting $y' = f(t, y)$ and

$$y'' = \frac{\partial f}{\partial t}(t_0, y(t_0)) + \frac{\partial f}{\partial y}(t_0, y(t_0)) \cdot f(t_0, y(t_0)) \tag{3.1.6}$$

into the Taylor expansion, the error of the Euler method is given by the difference of the algorithmic definition of the Euler method and the analytical Taylor expansion:

$$\frac{1}{2}h^2 \left[\frac{\partial f}{\partial t}(t_0, y(t_0)) + \frac{\partial f}{\partial y}(t_0, y(t_0)) \cdot f(t_0, y(t_0)) \right] + O(h^3)\,. \tag{3.1.7}$$

For the fourth-order Runge-Kutta method the numerical error is of order h^5 [11].
In the following, a gyration motion was used to check the quality of these two ODE solvers. For this test one uses a centripetal force, which holds the mass point on a circular path according to the formula:

$$F = -\frac{v^2}{r}\,. \tag{3.1.8}$$

After finishing one turn the mass point should reach the starting point again. Due to the accumulation of the numerical errors over the large number of time steps the starting point will not exactly be reached. This error after each turn can be measured and can be used to quantify the quality of the solver.

In figure 3.2 the error of the integration schemes are plotted as a function of the number of turns. As expected, the Runge-Kutta method is more precise than the Euler method. The error of the Euler method increases with the number of steps. For the Runge-Kutta method it oscillates at very low values.
Another test of the ODE solver is to vary the time step for the same centripetal movement and check the conservation of energy. If the variation was more than one

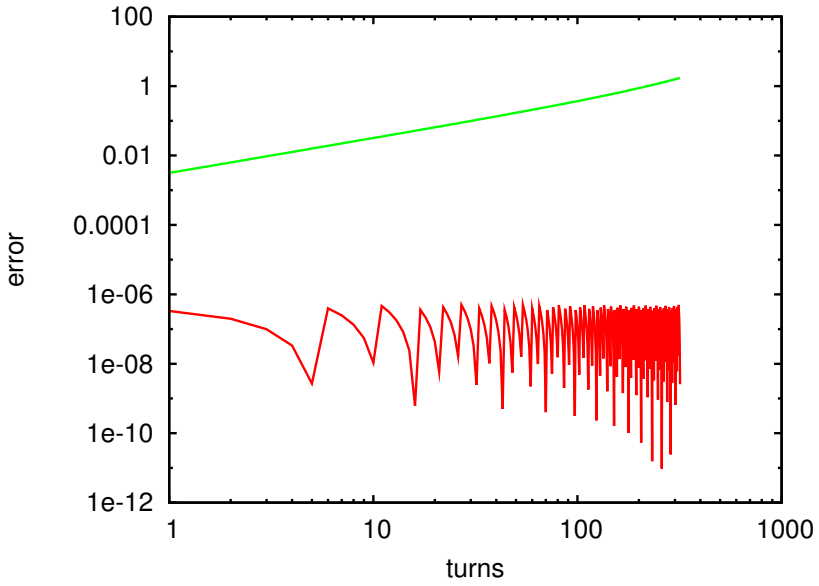

Figure 3.2: numerical error as a function of number of turns for Euler (green) and Runge-Kutta (red)

percent of the starting energy, the integration was stopped. This stopping time can be used to compare energy conservation of the two approaches. The result is plotted in figure 3.3. To reach the same total run-time with energy conservation, the Euler method needs a much smaller time step than the Runge-Kutta method. So, for the same time step the Runge-Kutta method guarantees a better energy conservation, which is a very big advantage of this method. Therefore, the Runge-Kutta algorithm allows longer times to be simulated while having better energy conservation.

3.2 Reduction of the system

Following the idea of Dullin [6] the system of the equations of motion is reduced to a much lower number of dimensions, reducing the workload for solving the problem numerically and allowing even analytical analysis. To do this an invariant set of equations will be introduced and the Hamiltonian and the corresponding equations of motion will then be solved. In order to find out, whether a system of equations is really defining an invariant of the system, one has to check the derivatives of the respective variables. To simplify the system the problem will reduced by the general assumption that the spin axis of the top is vertical and its center of mass is on the

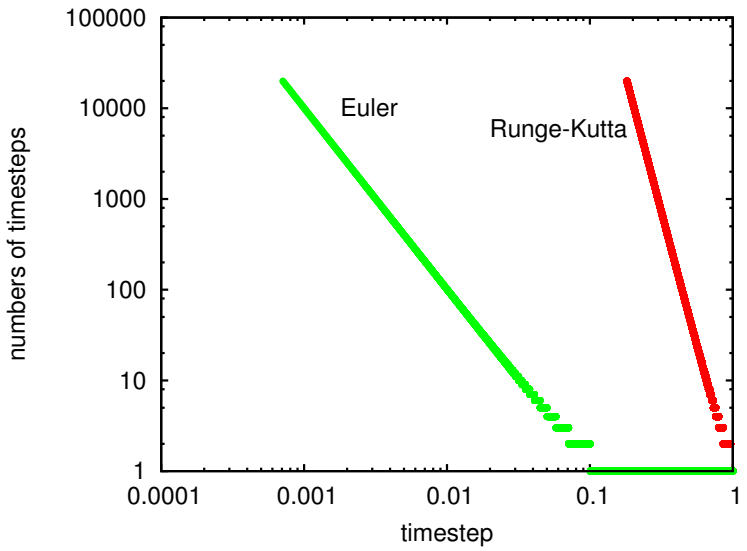

Figure 3.3: number of steps with energy conservation variation below one percent as a function of time step: green - Euler, red - Runge-Kutta

z-axis. This seems to be a good approximation according to the symmetry of the system, in other words the system is invariant under a torus action. Then the set $\mathcal{I}$ is given by:

$$\mathcal{I} = \{x = y = 0,\ \theta = \phi = 0,\ p_x = p_y = 0,\ p_\theta = p_\phi = 0\}\,. \tag{3.2.1}$$

To remove the singularity in the equations of motion from chapter 2.3 from $\frac{1}{\sin\theta}$ appearing for vertical orientation. This can be removed by a variable transformation following Dullin [6].
One introduces new angles with the following conventions. φ describes a rotation about the x-axis, ϑ about the y-axis and ζ about the z-axis of the laboratory coordinate system. So the transformation matrix is calculated as

$$\mathbf{R} = \mathbf{R}_x(\varphi)\mathbf{R}_y(\vartheta)\mathbf{R}_z(\zeta) \tag{3.2.2}$$

with three rotational matrices of the $\mathbb{R}^3$:

$$\mathbf{R}_x(\varphi) = \begin{pmatrix} 1 & 0 & 0 \\ 0 & \cos\varphi & \sin\varphi \\ 0 & -\sin\varphi & \cos\varphi \end{pmatrix} \tag{3.2.3}$$

$$\mathbf{R}_y(\vartheta) = \begin{pmatrix} \cos\vartheta & 0 & \sin\vartheta \\ 0 & 1 & 0 \\ -\sin\vartheta & 0 & \cos\vartheta \end{pmatrix} \tag{3.2.4}$$

$$\mathbf{R}_z(\zeta) = \begin{pmatrix} \cos\zeta & \sin\zeta & 0 \\ -\sin\zeta & \cos\zeta & 0 \\ 0 & 0 & 1 \end{pmatrix} \tag{3.2.5}$$

$$\mathbf{R}(\varphi,\vartheta,\zeta) = \begin{pmatrix} \cos\zeta\cos\vartheta & \sin\zeta\cos\vartheta & \sin\vartheta \\ -\sin\varphi\cos\zeta\sin\vartheta - \cos\varphi\sin\zeta & \cos\varphi\cos\zeta - \sin\varphi\sin\zeta\sin\vartheta & \sin\varphi\cos\vartheta \\ \sin\varphi\sin\zeta - \cos\varphi\cos\zeta\sin\vartheta & -\cos\varphi\sin\zeta\sin\vartheta - \sin\varphi\cos\zeta & \cos\varphi\cos\vartheta \end{pmatrix}. \tag{3.2.6}$$

To compute the expression for the rotational energy in the new coordinates, the angular velocity $\vec{\omega}$ is still missing. To evaluate it, the following steps have to be done. The change of the transformation matrix in laboratory coordinates has to be expressed in a base of the SO(3) group:

$$(\mathbf{R}^T \cdot \frac{d\mathbf{R}}{dt}) = \begin{pmatrix} 0 & \dot\varphi\sin\vartheta + \dot\zeta & -\dot\varphi\sin\zeta\cos\vartheta + \dot\vartheta\cos\zeta \\ -\dot\varphi\sin\vartheta - \dot\zeta & 0 & \dot\vartheta\sin\zeta + \dot\varphi\cos\zeta\cos\vartheta \\ \dot\varphi\sin\zeta\cos\vartheta - \dot\vartheta\cos\zeta & -\dot\vartheta\sin\zeta - \dot\varphi\cos\zeta\cos\vartheta & 0 \end{pmatrix}. \tag{3.2.7}$$

The base of the SO(3) group is given by [13]

$$S_1 = \begin{pmatrix} 0 & 0 & 0 \\ 0 & 0 & -1 \\ 0 & 1 & 0 \end{pmatrix} \qquad S_2 = \begin{pmatrix} 0 & 0 & 1 \\ 0 & 0 & 0 \\ -1 & 0 & 0 \end{pmatrix} \qquad S_3 = \begin{pmatrix} 0 & -1 & 0 \\ 1 & 0 & 0 \\ 0 & 0 & 0 \end{pmatrix}. \tag{3.2.8}$$

With the help of this base the vector components of the angular velocity can be identified from the matrix (3.2.7). Writing them as a vector gives:

$$\vec{\omega} = \begin{pmatrix} -\dot\vartheta\sin\zeta - \dot\varphi\cos\zeta\cos\vartheta \\ -\dot\varphi\sin\zeta\cos\vartheta + \dot\vartheta\cos\zeta \\ -\dot\varphi\sin\vartheta - \dot\zeta \end{pmatrix}. \tag{3.2.9}$$

With these calculations it is possible to express the rotational energy, which was the problem when trying to reduce the system, in these new variables:

$$T_{rot} = \frac{1}{2}\left[\left(\dot\varphi\sin\vartheta + \dot\zeta\right)^2 C + \left(\dot\zeta^2 + \dot\varphi^2\cos^2\vartheta\right) A\right]. \tag{3.2.10}$$

The whole Hamiltonian can then be written as:

$$\begin{aligned}\mathcal{H} =& \frac{1}{2m}\left(p_x^2 + p_y^2 + p_z^2\right) + \frac{1}{2}\left[\left(\dot{\varphi}\sin\vartheta + \dot{\zeta}\right)^2 C + \left(\dot{\zeta}^2 + \dot{\varphi}^2\cos^2\vartheta\right) A\right] \\ &+ \mu\left(\sin\vartheta B_x + \sin\varphi\cos\vartheta B_y + \cos\varphi\cos\vartheta B_z\right) + mgz\,. \end{aligned} \tag{3.2.11}$$

Now, the reduction can be done with the formulated invariant set of equations $\mathcal{I}$. This leads to a reduced form of the Hamiltonian:

$$H_{\mathcal{I}}(z,\psi,p_z,p_\psi) = \frac{p_z^2}{2m} + \frac{p_\psi^2}{2C} + \mu\Phi_1(z) + mgz\,. \tag{3.2.12}$$

Of course the derivatives of the variables that occur in the invariant set are all equal to zero. So the system of 12 dimensions can be reduced to a system of four degrees of freedom:

$$\begin{aligned} \dot{z} &= \frac{p_z}{m} & \dot{p_z} &= -U_z(0,0,z,0,0) \\ \dot{\psi} &= \frac{p_\psi}{C} \equiv \sigma & \dot{p_\psi} &= 0\,. \end{aligned}$$

The spin rate of the top is defined as σ and is constant for the invariant set. With the ODE solvers, which were introduced above, these equations of motion can be integrated and the solutions can be plotted. For the variable z one gets the phase portrait shown in figure 3.4. One can realize that there are stable trajectories.

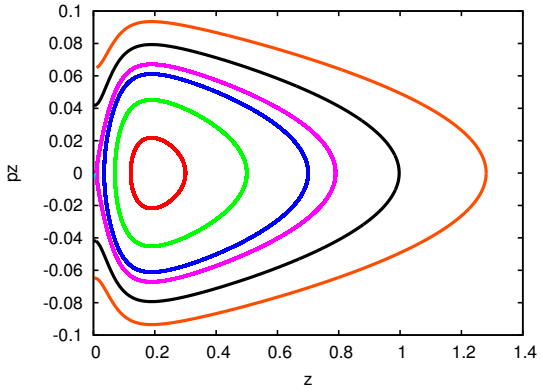

Figure 3.4: phase space $p_z(z)$, every color represents another energy

3.3 Stability and Linearization

The potential from the reduced Hamiltonian is given by:

$$U_{\mathcal{I}} = mgz + \mu\Phi_1(z)\,. \tag{3.3.1}$$

To find an equilibrium condition for z the potential has to be differentiated with respect to z and the roots of this equation are needed:

$$U'_{\mathcal{I}}(z) = mg + \mu\Phi_2(z) = 0\,. \tag{3.3.2}$$

We can visualize this equation by plotting both terms and search for intersection points:

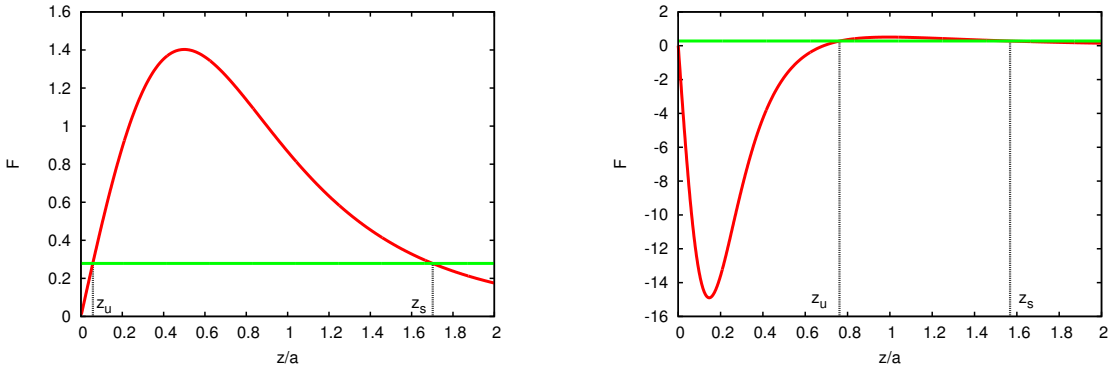

Figure 3.5: equilibrium condition for z: green - mg, red - $-\mu\Phi_2$
left: without hole, right: with hole

Dullin [6] calculated a base plate without a hole. In this work the simulations reflect a toy levitron with a hole in the base plate. The top weighs 28,4g, which is lower than the mass of Dullin's top. Therefore, the line of the gravitational force mg is at greater values resulting in different intersection points where the forces balance. For the base plate of radius 10cm with a hole of 3cm these equilibrium points are at 7,62cm and 15,68cm. There are huge differences for small z between the cases, where the base plate is taken without a hole and the one with a hole, but for larger z the differences get smaller (figure 3.6).

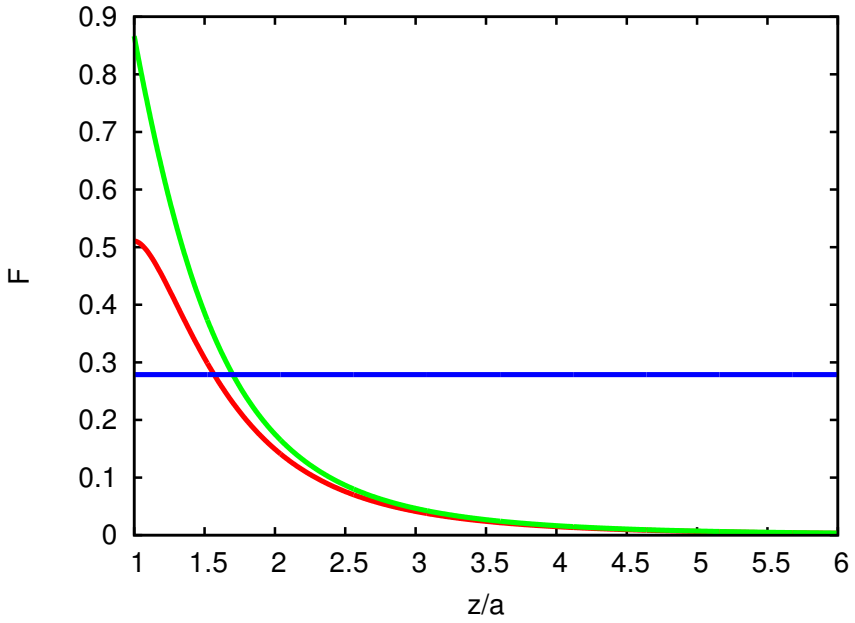

Figure 3.6: forces for larger z: blue - gravitational force, red - magnetic force with hole, green - magnetic force without hole

For a stable solution, the position of the top should be in a potential minimum, thus the second derivative has to be greater than zero, so:

$$U_{\mathcal{I}}''(z) = \mu\Phi_3(z) > 0\,. \tag{3.3.3}$$

So the first intersection point is an unstable solution at z_u, the second intersection point is a stable solution for equilibrium at z_s. Notice that in figure 3.5 $-\mu\Phi_2(z)$ was plotted. Due to the different masses of the top, Dullin gets a lower stable point compared to this work. For the stable solution, one can write the z-dependence of the system in the following way:

$$z = z_s \qquad \dot{z} = 0\,. \tag{3.3.4}$$

For ζ it looks like:

$$\zeta = \sigma t \qquad p_\zeta = \sigma C\,. \tag{3.3.5}$$

The eight degrees of freedom, which are left, can be calculated from the Hamiltonian

from equation (2.3). Afterwards the system can be linearized and written as follows:

$$\begin{aligned}
\Delta\dot{x} &= \frac{1}{m}\Delta p_x \\
\Delta\dot{y} &= \frac{1}{m}\Delta p_y \\
\Delta\dot{\vartheta} &= \frac{1}{A}\Delta p_\vartheta \\
\Delta\dot{\varphi} &= -\frac{p_\zeta}{A}\Delta\vartheta + \frac{1}{A}\Delta p_\varphi \\
\Delta\dot{p}_x &= \frac{\mu\Phi_3}{2}\Delta x + \frac{\mu\Phi_2}{2}\Delta\vartheta \\
\Delta\dot{p}_y &= \frac{\mu\Phi_3}{2}\Delta y + \frac{\mu\Phi_2}{2}\Delta\varphi \\
\Delta\dot{p}_\vartheta &= \frac{\mu\Phi_2}{2}\Delta x + \left(\mu\Phi_1 - \frac{p_\zeta^2}{A}\right)\Delta\vartheta + \frac{p_\zeta}{A}\Delta p_\varphi \\
\Delta\dot{p}_\varphi &= \frac{\mu\Phi_2}{2}\Delta y + \mu\Phi_1\Delta\varphi\,.
\end{aligned}$$

Obviously, Dullin had some typos in his publication with wrong signs in these expressions. But the final results are in agreement. Defining two complex variables $u = \Delta x + \mathrm{i}\Delta y$ and $v = \Delta\vartheta + \mathrm{i}\Delta\varphi$ the system can be converted into an equation of the form $\ddot{w} = \mathbf{A}w + \mathbf{B}\dot{w}$:

$$\begin{pmatrix}\ddot{u}\\ \ddot{v}\end{pmatrix} = \begin{pmatrix}\frac{\mu\Phi_3}{2m} & \frac{\mu\Phi_2}{2m}\\ \frac{\mu\Phi_2}{2A} & \frac{\mu\Phi_1}{A}\end{pmatrix}\begin{pmatrix}u\\ v\end{pmatrix} + \begin{pmatrix}0 & 0\\ 0 & -\mathrm{i}\sigma\frac{C}{A}\end{pmatrix}\begin{pmatrix}\dot{u}\\ \dot{v}\end{pmatrix}\,. \tag{3.3.6}$$

Such an equation is solved by the ansatz $w(t) = w_0\mathrm{e}^{\lambda t}$, yielding:

$$w_0\lambda^2\mathrm{e}^{\lambda t} = Aw_0\mathrm{e}^{\lambda t} + Bw_0\lambda\mathrm{e}^{\lambda t}\,. \tag{3.3.7}$$

Dividing both sides by $w_0\mathrm{e}^{\lambda t}$ and move the left term to the right, one gets:

$$\mathbf{A} + \lambda\mathbf{B} - \lambda^2\mathbf{1} = 0\,. \tag{3.3.8}$$

To solve this equation one has to calculate the determinant, leading to the following polynomial expression:

$$P(\lambda) = \lambda^4 - \mathrm{i}\sigma\varrho\lambda^3 - \mu\left(\frac{\Phi_1}{A} + \frac{\Phi_3}{2m}\right)\lambda^2 + \mathrm{i}\sigma\varrho\mu\frac{\Phi_3}{2m}\lambda + \mu\frac{2\Phi_1\phi_3 - \Phi_2^2}{4mA}\,. \tag{3.3.9}$$

This polynomial has to be zero for stable solutions. ϱ is the quotient of the moments of inertia $\frac{C}{A}$ and the Φ_i are computed at the stable point in z direction z_s. This polynomial can be transformed into a more manageable form by substituting $\lambda = \mathrm{i}\sigma\varrho t$ and dividing by $(\sigma\varrho)^4$. Furthermore the following identities should be introduced [6]:

$$g_1 = \frac{\mu\Phi_1(z_s)}{\sigma^2\varrho^2 A} \qquad g_2 = \frac{\mu\Phi_2(z_s)}{2\sigma^2\varrho^2\sqrt{mA}} \qquad g_3 = \frac{\mu\Phi_3(z_s)}{2\sigma^2\varrho^2 m}\,. \tag{3.3.10}$$

So one gets the following polynomial in t:

$$N(t) = t^4 - t^3 + (g_1 + g_3)t^2 - g_3 t + g_1 g_3 - g_2^2\,. \tag{3.3.11}$$

To guarantee stability the stability condition from equation (3.3.2) for z movements must be fulfilled and the polynomial $N(t)$ has to have four real roots [6]. In other words, one has to search for coefficients for which the discriminant $G(g_1, g_2, g_3)$ of $N(t)$ is equal zero. For a polynomial of order four the computational software Mathematica computed the discriminant

$$\begin{aligned} G(g_1,g_2,g_3) =& 16g_1g_3^5 - 4g_3^5 - 16g_2^2g_3^4 - 64g_1^2g_3^4 + 48g_1g_3^4 - 8g_3^4 + 192g_1g_2^2g_3^3 - 60g_2^2g_3^3 \\ &+ 96g_1^3g_3^3 - 88g_1^2g_3^3 + 32g_1g_3^3 - 4g_3^3 - 128g_2^4g_3^2 - 352g_1^2g_2^2g_3^2 \\ &+ 124g_1g_2^2g_3^2 - 12g_2^2g_3^2 - 64g_1^4g_3^2 + 48g_1^3g_3^2 - 8g_1^2g_3^2 + 512g_1g_2^4g_3 \\ &- 48g_2^4g_3 + 192g_1^3g_2^2g_3 - 196g_1^2g_2^2g_3 + 36g_1g_2^2g_3 + 16g_1^5g_3 - 4g_1^4g_3 \\ &- 256g_2^6 - 128g_1^2g_2^4 + 144g_1g_2^4 - 27g_2^4 - 16g_1^4g_2^2 + 4g_1^3g_2^2\,. \end{aligned} \tag{3.3.12}$$

The g_i have to fulfill further constraints. For equilibrium in z direction $\mu\Phi_2 = -mg$ and since g_2 is proportional to $\mu\Phi_2$ it must be fulfilled that $g_2 < 0$. For vertical stability the inequality $\mu\Phi_3 > 0$ has to be satisfied, hence $g_3 > 0$. As mentioned earlier in this work, the magnetic field is pointing upwards on the z-axis, so $-\Phi_1 > 0$ and following $g_1 > 0$.

The next step will be to compute the critical spin rates for stable solutions following the approach of Dullin [6]. The space of all possible g_i is defined as a coefficient space and the subset G is the set, where $N(t)$ has four real roots. A change of the spin rate determines a ray through the origin in coefficient space. Then, the critical spin rates are simply the points where the ray intersects the subset G of the coefficient space. For points inside G and on the ray one gets a relative equilibrium. The ray is described by $l(g_1, g_2, g_3)$ with l a real parameter. Therefore the critical spin rates

were given by special values of l. These values can be calculated by setting the polynomial $L(l)$ equal zero:

$$L(l) = G(lg_1, lg_2, lg_3) \stackrel{!}{=} 0\,. \tag{3.3.13}$$

To eliminate the trivial solution $l = 0$, one can divide the equation by l^3 and get an polynomial of order three. To solve this the variables $g_{21} = -\frac{g_2}{g_1}$, $g_{31} = -\frac{g_3}{g_1}$ and α, which is an effective length and is calculated by $\sqrt{\frac{A}{m}}$, are introduced:

$$g_{21} = -\alpha\frac{\Phi_2(z_s)}{2\Phi_1(z_s)} \qquad g_{31} = -\alpha^2\frac{\Phi_3(z_s)}{2\Phi_1(z_s)}\,. \tag{3.3.14}$$

A position z can be found for which Φ_3 is equal zero, so that the vertical equilibrium is assured. z_c is associated with the maximum weight of the top at which this vertical equilibrium is still assured. Then it follows, that

$$g_{21} = -\alpha\frac{\Phi_2(z_c)}{2\Phi_1(z_c)} < \frac{1}{\sqrt{12}}\,. \tag{3.3.15}$$

Now the polynomial equation $L(l) = 0$ can be written by dividing by l in the following way:

$$L(l, g_{31} = 0) = -16(4g_{21}^2 + 1)^2 l^2 + (144g_{21} + 4)l - 27g_{21}^2\,. \tag{3.3.16}$$

To simplify the solutions one can make the approximation of small g_{21} and use the Taylor series. Then the solutions are given by:

$$l_1 = \frac{1}{4}(1 + g_{21}^2) \approx \frac{1}{4} \tag{3.3.17}$$

$$l_2 = \frac{27}{4}g_{21}^2 \tag{3.3.18}$$

Now these values for l must be transformed into values for the critical spin rates σ_i. For this one has to look at the definition of g_2 in equation (3.3.10) and use the equilibrium condition $-mg = \mu\Phi_2$:

$$g_2 = \frac{\mu\Phi_2}{2\sigma^2\varrho^2\sqrt{mA}} = \frac{-g}{2\sigma^2\varrho^2\alpha} = \frac{-gA}{2\sigma^2\varrho C\alpha} = \frac{-mg\alpha^2}{2\sigma^2\varrho C\alpha}\,. \tag{3.3.19}$$

Solving this equation for σ^2 gives:

$$\sigma^2 = -\frac{mg\alpha}{2\varrho g_2 C}\,. \tag{3.3.20}$$

Setting the critical value $-l_i g_{21}$ for g_2 one gets:

$$\sigma_i^2 = \frac{mg\alpha}{2\varrho l_i g_{21} C} = \frac{gA}{2\varrho l_i g_{21}\alpha C} = \frac{g}{2\varrho^2 l_i g_{21}\alpha} = \frac{-g\Phi_1}{\varrho^2 l_i \alpha^2 \Phi_2}\,. \tag{3.3.21}$$

For the last step it is used that $g_{21} = -\frac{\alpha\Phi_2}{2\Phi_1}$. Including z_c for which $\Phi_3 = 0$ one gets for the first critical spin rate:

$$\sigma_1 \approx -4\frac{g\Phi_1(z_c)}{\Phi_2(z_c)\alpha^2\varrho^2}\,. \tag{3.3.22}$$

The second spin rate can be written as follows:

$$\sigma_2 \approx -\frac{4g\Phi_1(z_c)}{27g_{21}^2\alpha^2\varrho^2\Phi_2(z_c)} = -\frac{16\Phi_1^3 g}{27\alpha^4\Phi_2^3\varrho^2} = \frac{16}{27}\left(\frac{-\Phi_1}{\Phi_2}\right)^3\frac{g}{\alpha^4\varrho^2}\,. \tag{3.3.23}$$

The critical spin rates as a function of g_{21} are shown in figure 3.7

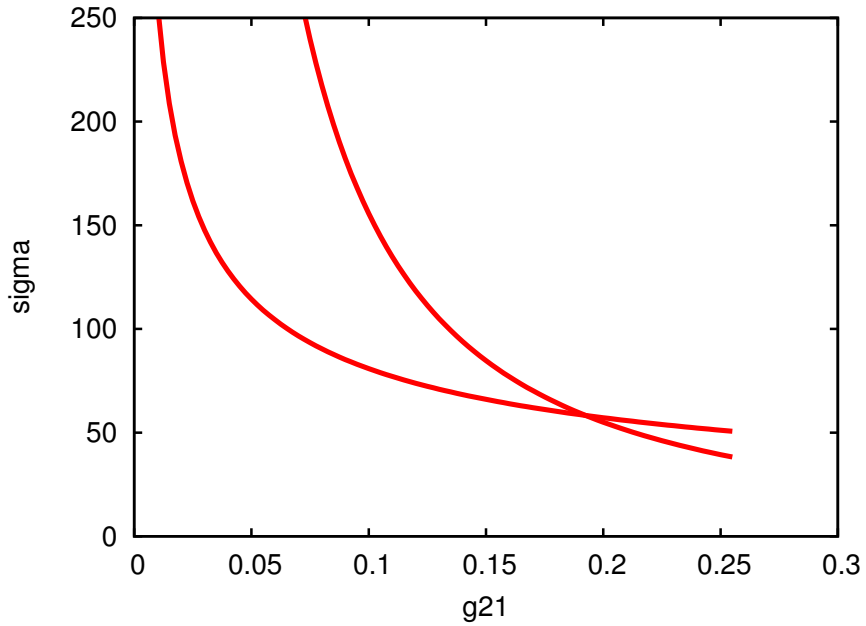

Figure 3.7: critical spin rates as a function of $g_2 1$

At point z_c one gets $\frac{\sigma_1}{2\pi} \approx 17\text{Hz}$ [6]. This is nearly the same as one can measure

in experiments [9]. One can compare these results with numerical analysis scanning the tilt and the spin rate for stable trajectories [5]. The results of this approach are shown in figure 3.8 and show similar values of spin and tilt rates as presented before.

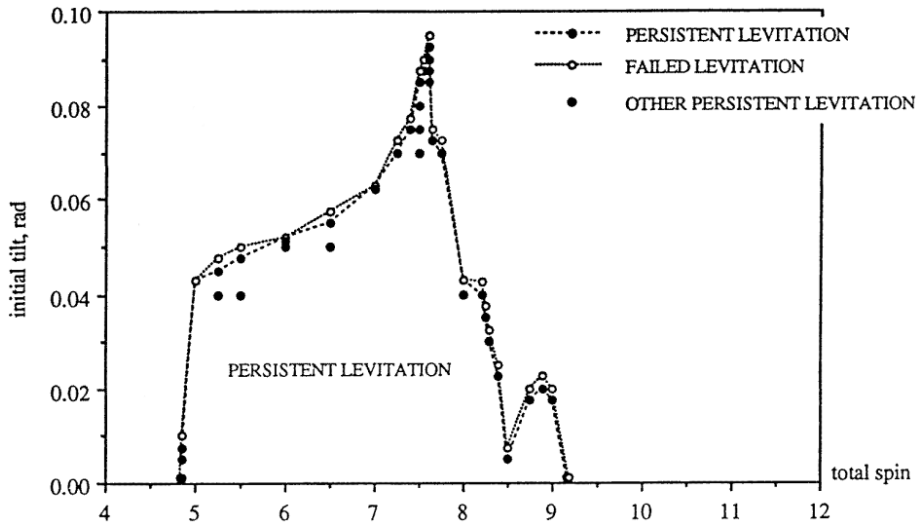

Figure 3.8: stable solutions as a function of spin and tilt [5]

To get persistent levitation it is necessary to have a small tilt and a convenient spin rate, here expressed in a normed parameter connected with the spin rate. It is important to realize that too large tilts as well as a too fast or too slow spinning of the top leads to unstable trajectories.

4 Conclusions

The goal of the work was to examine the physics of a levitron. Following classical mechanics one can formulate the equations of motion from the Hamiltonian. To simplify the analytical solutions, an invariant of the system was introduced. For this invariant set of equations the Hamiltonian was reduced. Using a linearization approach the stability of the system was analyzed. The comparison of critical spin rates obtained with this approach agreed with other numerical scans from literature. The theory of a levitating top is as challenging as playing with it as a physical toy.

Acknowledgements

Writing a scientific thesis for the first time causes a lot of problems, even some, one would not imagine from the beginning. Because of that at the end of this thesis I want to thank all people, who helped me to finish my work.
First of all I want to express my gratitude to my supervisor Prof. Dr. Ralf Schneider for his great support, his endless patience while discussing trivialities with me and for the daily hot chocolate. Furthermore, I want to thank the members of the COMAS group, especially Gunnar, Tim and Lars for helping me to improve my English. A special thank to Robert Warmbier for some important tips in programming. A special thank also to Matthias, who helped me to solve some computing problems.
I am grateful to my girl friend Karo for encouraging me in some depressing periods of the work. Moreover, she and my friends Basti and Anni made it possible to do some funny experiments during the breaks and to produce some avocation.
I would like to thank my parents for their never-ending trust and support.

Bibliography

[1] "Le levitron ou l'anti-gravité révélée." `http://www.amusoire.net/?2005/04/20/58-la-gravite-on-peut-leviter` [Online; accessed 15-May-2011].

[2] T. Bergeman, G. Erez, and H. Metcalf, "Magnetostatic trapping fields for neutral atoms," *Physical Review A*, vol. 35, no. 4, p. 1535, 1987.

[3] M. Berry, "The levitron tm: an adiabatic trap for spins," *Proceedings: Mathematical, Physical and Engineering Sciences*, vol. 452, no. 1948, pp. 1207–1220, 1996.

[4] T. Jones, M. Washizu, and R. Gans, "Simple theory for the levitron," *Journal of applied physics*, vol. 82, p. 883, 1997.

[5] R. F. Gans, T. B. Jones, and M. Washizu, "Dynamics of the levitron tm," *Journal of Physics D: Applied Physics*, vol. 31, no. 6, p. 671, 1998.

[6] H. Dullin and R. Easton, "Stability of levitrons," *Physica D: Nonlinear Phenomena*, vol. 126, no. 1-2, pp. 1–17, 1999.

[7] H. Goldstein, *Klassische Mechanik, Wiesbaden, 6.* Akademische Verlagsgesellschaft, 1981.

[8] W. Wessner, *Mesh Refinement Techniques for TCAD Tools.* PhD thesis, Technische Universität Wien, November 2006.

[9] M. Simon, L. Heflinger, and S. Ridgway, "Spin stabilized magnetic levitation."

[10] J. Jackson, *Klassische Elektrodynamik, de Grutyer 1983, 2.* Aufl, 2 ed., 1983.

[11] P. DeVries, *A first course in computational physics.* John Wiley & Sons, 1994.

[12] "euler method." `http://upload.wikimedia.org/wikipedia/commons/a/ae/Euler_method.png` [Online; accessed 13-June-2011].

[13] I. Bronstein, K. Semendjajew, G. Musiol, and H. Mühlig, *Taschenbuch der Mathematik*. Harri Deutsch Verlag, 2008.